

## Evaluation of Intracranial Aneurysms with 3T TOF MRA: Compared to 64-MDCTA

Y. Hiratsuka<sup>1</sup>, H. Miki<sup>1</sup>, K. Kikuchi<sup>1</sup>, I. Kiriya<sup>1</sup>, T. Mochizuki<sup>1</sup>, S. Takahashi<sup>2</sup>, I. Matsubara<sup>3</sup>, and K. Sadamoto<sup>3</sup>

<sup>1</sup>Department of Radiology, Ehime University School of Medicine, Toon, Ehime, Japan, <sup>2</sup>Department of Radiology, Washo-kai Sadamoto Hospital, Matsuyama, Ehime, Japan, <sup>3</sup>Department of Neurosurgery, Washo-kai Sadamoto Hospital, Matsuyama, Ehime, Japan

**Introduction:** MR Angiography (MRA) and CT Angiography (CTA) are generally known as representative methods for a diagnosis of intracranial aneurysms. These modalities enable us to understand their locations, shape, and relationships to surrounding structures without an invasion. Development and improvement of new CT/MRI system have produced a better diagnostic quality, and are expected to change the diagnosis of aneurysms. The purpose of this study is to compare 3-tesla (3T) 3D time-of flight (TOF) MRA and 64-row CTA (MDCTA) using volume-rendering (VR) images for the evaluation of the intracranial aneurysms, adjacent small arteries, and their relationships.

**Materials and Methods:** Twenty-two patients (11 men and 11 women; age range, 35-78 years; mean age, 62.09 years) with 25 aneurysms (all non-ruptured) suspected on 3T TOF MRA. MDCTA with 64-row and 3D digital angiography (DA) were also performed consecutively. The size of the aneurysms was; <3mm: one lesion, 3mm to 5mm: eight lesions, more than 5mm ≤ : 16 lesions (7mm ≤ : five lesions). The locations of aneurysms were as follows: anterior-communicating artery: five lesions, middle cerebral artery: five lesions, posterior communicating artery: four lesions, vertebral and basilar artery: four lesions and internal carotid artery: seven lesions. MR examinations were performed on 3T MRI with eight-element phased array coil. Imaging parameters for 3D TOF MRA were as follows: 512x224matrix (512reconstructed), with parallel imaging (ASSET factor 2.0), TR/TE: 25/3.1ms, a ramped radio-frequency pulse with a central flip angle of 20°, one slab of 90sections, bandwidth: 31.2kHz, FOV: 190x170mm, NEX: 1, and 1.0-mm-thick (ZIP2 0.5mm). MDCTA examinations were performed with following parameters; 120kV, auto mA (max 500mA), pitch 0.531, and rotation time 0.40sec/rot. Nonionic iodinated contrast mediums (300 mgI/ml, 50ml) were injected with a power injector at a rate of 3.5ml/sec, and a scan delay was individually adapted by using a bolus-tracking technique. DA examinations were performed after MRA and CTA examination using a 3D DA angiographic unit with a flat panel detector. Nonionic iodinated contrast medium (350mgI/ml, 6-8ml) was injected into the internal carotid or vertebral artery with a power injector at a rate of 4-6ml/sec while scanning. The each data was transferred to a post-processing workstation and the VR images were generated with an adequate threshold on each study. The VR images were evaluated on a display by two radiologists, and 3D-DA images were used as a standard of reference. The original grading scale was applied for evaluation, and examination items were as follows; the detection of aneurysms, the relationship to parental arteries, the aneurysmal shape, the bleb formations, and the adjacent small arteries using original grading score. A statistical significance between MRA and CTA were assessed with a paired-t test or a Wilcoxon signed-ranks test (P value < 0.05).

**Results:** All aneurysms were detected exactly on both methods, and the relationships to parental arteries were also clearly identified in all cases (Fig 1.). In the evaluation for the shape of aneurysms, there was no significant difference between two methods. As the depiction of bleb formations, the MRA-VR images had a higher sensitivity and small number of false negative cases than CTA. However, many of false positive cases were also found on MRA (Fig 2.). In the evaluation of the adjacent small arteries, the MRA-VR images with the adequate threshold had the same quality for diagnosis of the small adjacent arteries compared to the CTA-VR images (Fig 3).

**Conclusions:** 3T TOF MRA has almost the same ability for the detection and evaluation of intracranial aneurysms and the surrounding small arteries compared to MDCTA. Therefore, the improvement of diagnosis on 3T TOF MRA will decrease the additional CTA examination after MRA.

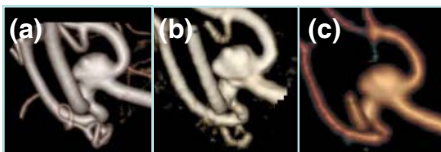


Fig 1. 53M Lt. MCA AN (5.3mm)  
(a)DA-VR, (b)MRA-VR, (c)CTA-VR  
The AN and parental artery were depicted with the same quality as DA.

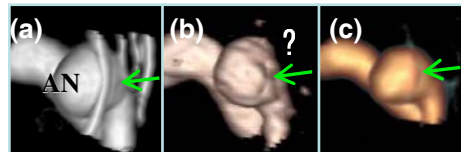


Fig 2. 70M Rt. MCA AN (6.5mm);  
(a) DA-VR, (b) MRA-VR, (c) CTA-VR  
MRA showed the bleb-like lesion on the aneurysmal surface (green arrow). It was not depicted on DA and CTA.

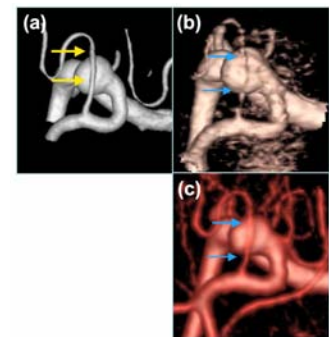


Fig 3. 70M Rt. MCA AN (6.2mm);  
(a) DA -VR, (b) MRA-VR, and (c) CTA-VR  
The small artery was depicted on the DA-VR images (yellow arrows), and also depicted clearly on MRA and CTA-VR images with the adequate threshold (blue arrows).